Nailfold Microvascular Imaging by Dynamic Optical Coherence Tomography in Systemic Sclerosis: A Case-Controlled Pilot Study

JID Open

Giuseppina Abignano[1,2,3], Lorraine Green[1,2], Sookhoe Eng[1,2], Paul Emery[1,2] and Francesco Del Galdo[1,2]

In systemic sclerosis, outcome measures of skin microvasculopathy are needed for both clinical trials and practice. The aim of this study was to determine whether dynamic-optical coherence tomography (D-OCT) is able to provide information on microvasculopathy compared with the current gold standard, nailfold video-capillaroscopy (NVC), in patients with systemic sclerosis. This case-controlled study included (i) 40 patients with systemic sclerosis, classified by NVC pattern in four age- and sex-matched groups (normal/nonspecific, early, active, late); (ii) a fifth group of 10 age- and sex-matched healthy controls. All participants underwent NVC and D-OCT. D-OCT images were compared with the corresponding NVC images. Reliability was assessed. D-OCT images visualized the corresponding NVC patterns. D-OCT microvascular flow density was different across the five NVC pattern groups ($P = 0.0114$) with a significant trend test ($P = 0.0006$). Microvascular flow density correlated with the NVC semiquantitative score ($r = -0.7$, $P < 0.0001$), number of abnormal shapes/mm ($r = -0.3$, $P = 0.0264$), and number of capillaries/mm ($r = 0.6$, $P < 0.0001$). Reliability was excellent (intraclass correlation coefficient > 0.9). In conclusion, in patients with systemic sclerosis, D-OCT provided qualitative and quantitative information on nailfold microvasculopathy, showing a correlation between microvascular flow density and NVC scores. The development of D-OCT as a standardized imaging technique could provide a quantitative outcome measure in clinical trials and practice.

Journal of Investigative Dermatology (2022) **142,** 1050–1057; doi:10.1016/j.jid.2021.08.436

INTRODUCTION

Systemic sclerosis (SSc) is a complex disease characterized by early microvascular abnormalities, immune dysregulation and chronic inflammation, and subsequent fibrosis of the skin and internal organs (Varga et al., 2017). Several imaging techniques have been adopted over the past years to assess microvasculopathy in patients with SSc (Barsotti et al., 2020; Bukhari et al., 2000; Cutolo et al., 2000; Della Rossa et al., 2013; Maricq et al., 1980; Rosato et al., 2011; Sulli et al., 2008). Nailfold videocapillaroscopy (NVC) is the current gold standard to detect microvascular changes at the nailfold of patients with SSc (Bukhari et al., 2000; Cutolo et al., 2000; Smith et al., 2020, 2019), and NVC pattern abnormalities are included in the very early diagnosis of SSc (Avouac et al., 2011; LeRoy and Medsger, 2001) and in the 2013 American College of Rheumatology/European League Against Rheumatism SSc classification criteria (van den Hoogen et al., 2013). Over the past years, several scoring systems have been developed to quantify NVC changes (Avouac et al., 2017; Cutolo et al., 2016; Sulli et al., 2008). However, to integrate microvascular status evaluation with measurement of blood flow in SSc, a number of studies have investigated various other techniques able to assess and quantify cutaneous blood perfusion, including laser Doppler imaging and laser speckle contrast analysis (Barsotti et al., 2020; Cutolo et al., 2018; Della Rossa et al., 2013; Melsens et al., 2020; Rosato et al., 2011). Within this group, a promising tool is the dynamic-optical coherence tomography (OCT) (D-OCT), a newly developed OCT technology. In addition to the images of traditional OCT scan, D-OCT enables the visualization of flow within the cutaneous microvasculature through the detection of rapid changes in the interferometric signal of blood flow (Olsen et al., 2018b; Ulrich et al., 2016).

Traditional OCT has a 20-year history of application in dermatology (Abignano et al., 2019b, 2017; Aydin et al., 2013; Welzel et al., 1997) and has been used over the recent years as, to our knowledge, a previously unreported imaging technique able to provide a virtual biopsy of the examined skin sample in patients with SSc (Abignano and Del Galdo, 2020, 2014; Abignano et al., 2013; Kang et al., 2014; Pires et al., 2018; Ring et al., 2015; Su et al., 2015). It uses infrared light and is able to produce sample images of micron resolution. Previous studies have used traditional OCT to evaluate fibrotic aspects of SSc skin, showing that the

[1]*Leeds Institute of Rheumatic and Musculoskeletal Medicine, School of Medicine, University of Leeds, Leeds, United Kingdom;* [2]*NIHR Leeds Biomedical Research Centre, Leeds Teaching Hospitals NHS Trust, Leeds, United Kingdom; and* [3]*Rheumatology Institute of Lucania (IReL) and Rheumatology Department of Lucania, San Carlo Regional Hospital, Potenza, Italy*

Correspondence: Giuseppina Abignano, Rheumatology Institute of Lucania (IReL), San Carlo Regional Hospital, Via Potito Petrone snc, 85100 Potenza, Italy. E-mail: g.abignano@hotmail.com

Abbreviations: D-OCT, dynamic-optical coherence tomography; HC, healthy control; MVFD, microvascular flow density; NVC, nailfold video-capillaroscopy; OCT, optical coherence tomography; SSc, systemic sclerosis

Received 23 November 2020; revised 21 June 2021; accepted 8 August 2021; accepted manuscript published online 25 September 2021; corrected proof published online 23 October 2021

measured optical density correlated with the severity of skin involvement at the site of analysis and with histopathology findings (Abignano et al., 2013; Pires et al., 2018). It was also shown that OCT was a reliable technique (Abignano et al., 2013). Over the past few years, there have been growing interest and efforts to enable OCT to study the microcirculation of human skin, including the nail fold (An et al., 2010; Choi et al., 2014).

A recent multicentre study carried out by a group of dermatologists with expertise in OCT explored the value of D-OCT for imaging of skin blood flow in healthy subjects and showed that D-OCT was able to reliably image and identify changes in the skin vasculature consistent with the induced physiological blood flow changes (Themstrup et al., 2016b). They also validated the D-OCT technique as an imaging tool of the vascular networks in healthy skin by comparing the results with those of already accepted blood flow measuring tools such as laser speckle contrast analysis measurements on identical skin sites. Their findings supported the use of D-OCT imaging for in vivo microcirculation imaging of the skin (Themstrup et al., 2016b).

The potential application of nailfold D-OCT to patients with SSc has been recently reported (Deegan et al., 2018; Ring et al., 2016; Ulrich et al., 2016). In their four-case series, Ring et al. (2016) showed that D-OCT capillaroscopy was able to visualize the capillary morphology, the surrounding skin architecture, and flow status of the capillaries in the nail fold. In addition, they showed that D-OCT quantified changes of the blood flow in normal nailfold capillaries after application of nitroglycerine and brimonidine. However, they suggested that further studies were needed to validate and explore the usefulness of this imaging technology in the diagnosis and management of SSc and dermatomyositis (Ring et al., 2016). In this pilot study, we aimed to explore the use of D-OCT in comparison with that of NVC evaluation of nailfold capillaries in a larger group of patients with SSc classified by NVC pattern.

RESULTS

D-OCT correlates with videocapillaroscopy by qualitative analysis of nailfold images

Table 1 shows the clinical characteristics of the 40 patients with SSc (10 patients in each group of the four NVC patterns). Age and sex were not significantly different between the groups ($P > 0.05$). The mean age of the matched healthy controls (HCs) was 58.8 (± 5.4) years, eight were females, and two were males. The finger with the highest capillary score in patients with SSc was the fourth in 28 (70%), the fifth in six (15%), the third in five (12.5%), and the second in one (2.5%) patient. Within the SSc group without a scleroderma NVC pattern, the pattern was classified as normal in two (20%) patients and as nonspecific (presence of enlarged loops and/or microhemorrhages in eight (80%) patients. Each nailfold D-OCT scan lasted 60 seconds, was well-tolerated, and did not require the use of ultrasound gel or immersion oil. The same nailfold capillary features visualized using NVC were visualized with D-OCT en-face view images. The representative en-face view images are shown in Figure 1 and illustrate the correspondence of capillary loops, their distribution, their morphology, presence of hemorrhages, and the overall capillary pattern between the NVC and nailfold D-OCT. The NVC patterns of the enrolled subjects significantly correlated with the classification of the nailfold D-OCT images by the blinded OCT assessor ($r = 0.9$, $P < 0.0001$). Figure 2a and b shows the two representative nailfold areas scanned by D-OCT. Figure 2a and b also shows the several modalities used to analyze and measure each capillary parameter and area. In addition, the nailfold D-OCT was able to provide a three-plane view of the examined nailfold (Figure 2c). Altogether, the slices collected for each examined site provided a virtual vascular biopsy of the sample, amenable to different types of quantitative analysis.

Skin microvascular flow density at nailfold correlates with the semiquantitative and quantitative analysis of NVC

Quantitative analysis of D-OCT images indicated that the microvascular flow density (MVFD) was significantly different across three groups (HC, SSc with normal/nonspecific NVC patterns, and SSc with specific NVC patterns) ($P = 0.0046$) (Figure 3a). Further analysis showed a significant trend test result (slope = –0.03, $P = 0.0012$). When including the three specific NVC patterns in the analyses (early, active, late), there was an overall statistical significance across the five groups ($P = 0.0114$) (Figure 3b). Trend test analysis was significant (slope = –0.02, $P = 0.0006$). Quantification of MVFD showed a strong and significant negative correlation with semiquantitative NVC score (i.e., microangiopathy evolution score) ($r = -0.7$, $P < 0.0001$). Similarly, MVFD score correlated negatively with the number of abnormal shapes/mm ($r = -0.3$, $P = 0.0264$) and positively with the number of capillaries/mm ($r = 0.6$, $P < 0.0001$) (Figure 3c). MVFD score did not correlate with the number of giant capillaries/mm ($r = -0.2$, P = nonsignificant) and microhemorrhages/mm ($r = -0.2$, p = nonsignificant).

Reliability

The reliability of D-OCT was assessed in a subgroup of participants. The intraobserver reliability was assessed, and it showed an intraclass correlation coefficient of 0.975 (excellent), with a 95% confidence interval of 0.844–0.996. Most importantly, the MVFD score showed excellent interobserver reliability. Scores calculated by two assessors on the same nail fold on the same day showed an intraclass correlation coefficient of 0.926 (95% confidence interval of 0.617–0.987).

DISCUSSION

NVC has proven to give crucial insight into the microvascular environment of the skin of the digits. The technique has found a critical clinical value in SSc so much to become a crucial element in the classification criteria (Avouac et al., 2011; LeRoy and Medsger, 2001; van den Hoogen et al., 2013). Furthermore, NVC has shown a good clinical value in predicting severe vascular complications, including digital ulcers and pulmonary arterial hypertension in SSc (Caramaschi et al., 2007; Cutolo et al., 2016; Riccieri et al., 2013; Silva et al., 2015). In addition, the absence of scleroderma NVC pattern is valuable for the exclusion of SSc in unselected patients with Raynaud's phenomenon (Bissell et al., 2016). Nevertheless, the strong diagnostic value of NVC has not been paralleled by its use as an endpoint in clinical trials

Table 1. Clinical Features of Patients with Systemic Sclerosis Classified According to the NVC Pattern

Items	Normal/N-sp (n = 10)	Early (n = 10)	Active (n = 10)	Late (n = 10)
Sex (F/M), n	8/2	9/1	8/2	8/2
Age, years, mean (SD)	59.8 (9.4)	59 (10.1)	55 (12.3)	58.5 (8.9)
DD from 1st non-RP, y, mean (SD)	10.5 (9.9)	9.1 (10.8)	9.8 (7.3)	10 (10.2)
Diffuse SSc, n (%)	0 (0)	1 (10)	2 (20)	3 (30)
ANA+, n (%)	9 (90)	9 (90)	10 (100)	10 (100)
ACA+, n (%)	3 (30)	6 (60)	8 (80)	4 (40)
Antitopoisomerase I+, n (%)	1 (10)	3 (30)	1 (10)	4 (40)
AntiRNA pol III, n (%)	1 (10)	0 (0)	1 (10)	0 (0)
mRSS, median (IQR)	1 (0–1.25)	3 (0–7)	3 (0–4.25)	5 (3.5–11.8)
Teleangectasia, n (%)	3 (30)	4 (40)	9 (90)	3 (30)
Digital ulcers (current), n (%)	0 (0)	0 (0)	1 (10)	0 (0)
Fingertip pitting scars, n (%)	0 (0)	1 (10)	2 (20)	3 (30)
PAH, n (%)	0 (0)	1 (10)	1 (10)	0 (0)
ILD, n (%)	2 (20)	3 (30)	2 (20)	3 (30)
Calcium channel blockers, n (%)	3 (30)	4 (40)	2 (20)	4 (40)
ACE-inhibitors/ARB, n (%)	1 (10)	2 (20)	3 (30)	5 (50)
Sildenafil, n (%)	0 (0)	1 (10)	3 (30)	5 (50)
Bosentan, n (%)	0 (0)	0 (0)	1 (10)	1 (10)
Prostanoids, n (%)	0 (0)	0 (0)	2 (20)	1 (10)
Fluoxetine, n (%)	0 (0)	2 (20)	0 (0)	0 (0)
Antiaggregants, n (%)	2 (20)	1 (10)	1 (10)	3 (30)
Immunosuppressive therapy, n (%)	1 (10)	3 (30)	2 (20)	5 (50)

Abbreviations: ACA, anticentromere antibody; ACE, angiotensin-converting enzyme; ANA, antinuclear antibody; ARB, angiotensin receptor blocker; DD, disease duration; DLCO, diffusing capacity for carbon monoxide; F, female; FVC, forced vital capacity; ILD, interstitial lung disease; IQR, interquartile range; M, male; mRSS, modified Rodnan skin score; N-Sp, normal/nonspecific; NVC, nailfold videocapillaroscopy; PAH, pulmonary artery hypertension; RP, Raynaud's phenomenon; SSc, systemic sclerosis.

Table 1 includes four groups of patients with SSc, each with a different NVC pattern (normal/nonspecific [normal/N-sp], early, active, late). Continuous variables are expressed as mean ± SD (if normally distributed) and as median (IQR) (if not normally distributed); categorical data are expressed as number and percentage. Immunosuppressive therapy included mycophenolate (10 patients) and azathioprine (one patient in the NVC late-pattern group). Diagnosis of PAH was made at right heart catheterization when mean pulmonary arterial pressure was found to be ≥25 mm Hg and pulmonary arterial wedge pressure was found to be ≤15 mm Hg; ILD was defined by DLCO and FVC < 80% of the predicted value plus bibasilar fibrosis on chest high resolution computed tomography. Digital ulcer was defined clinically as a denuded area located on the fingers with loss of epithelialization and a break in the basement membrane, not located over the metacarpophalangeal joints and not associated with digital pitting scar or calcinosis.

mainly for the nature of its quantification. Although NVC offers a qualitative, semiquantitative, and quantitative assessment, it is only of the distal row of capillaries and does not offer insight into the morphology of deeper dermal vessels, the flow status of the capillaries, nor the architecture of the skin (Ring et al., 2016).

D-OCT has already been shown to be able to visualize the nailfold capillaries (Deegan et al., 2018; Ring et al., 2016; Ulrich et al., 2018). In this context, Ring et al (2016) first suggested the usefulness of D-OCT quantification by measuring changes in the blood flow in normal nailfold capillaries after application of nitroglycerine and brimonidine. In this study, building on the value of the microvasculature of the nail fold and the ability of D-OCT, we set out to perform a quantitative assessment of nailfold microvasculopathy by D-OCT in a well-characterized and phenotyped cohort of patients with SSc and a comparable HC group.

Although pilot in nature, our study supported the validity of D-OCT by the comparison with NVC as gold standard both at the qualitative level of pattern classification and at the quantitative level. In this pilot study, qualitative comparison of pattern classification between the two techniques showed a highly significant correlation, whereas quantitative analysis between MVFD and the single NVC parameters count showed a significant correlation only with a number of capillaries and, with a weaker significance, number of abnormal shapes. This is likely related to the fact that MVFD by D-OCT and NVC measure different aspects of microvasculopathy. In this study, MVFD measured overall dermal vessels flow density down to 0.6 mm depth, whereas the NVC count only assessed the distal row of capillaries. Therefore, used in combination with NVC, D-OCT could serve as a complementary tool to obtain additional information at the nail fold and potentially to assess and quantify microvasculopathy in other skin areas, as shown in HCs in previous studies (Themstrup et al., 2016b). The most significant and interesting aspect of MVFD, which deserves further investigation, is its correlation with the number of capillaries/mm because capillary density has been shown to be the most robust NVC risk factor for the development of new digital ulcers by previous studies (Caramaschi et al., 2007; Cutolo et al., 2016; Silva et al., 2015). The excellent reliability of the OCT technique was previously shown in patients with SSc using the same scanner (Abignano et al., 2013). In this study, we have shown that the dynamic function of OCT has an excellent intraobserver and interobserver reliability as well, making it an ideal assessment to offer a surrogate outcome measure of vasculopathy in SSc.

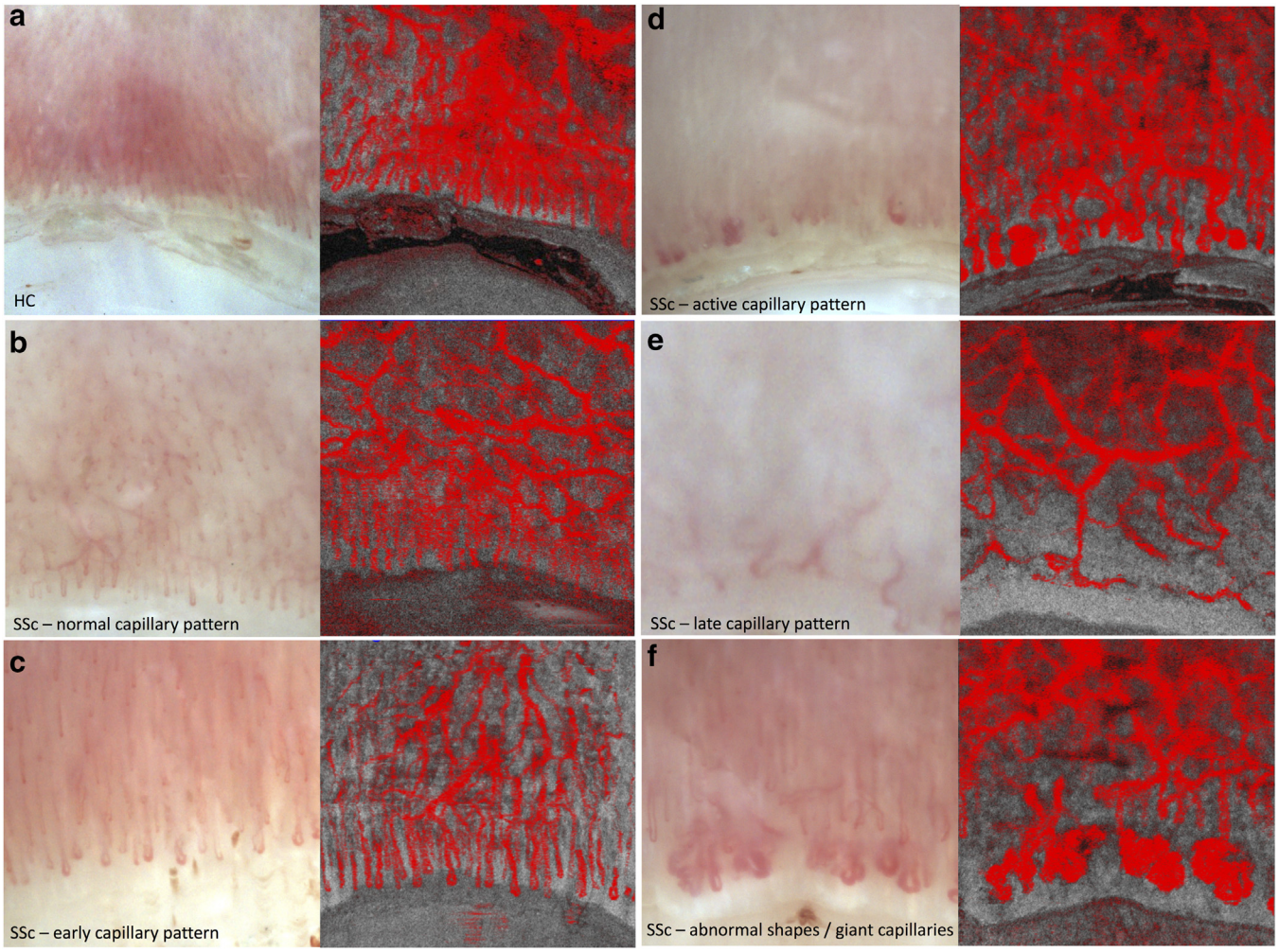

Figure 1. Representative images illustrate the correspondence of capillary loops, their distribution, morphology, presence of haemorrhages and the overall capillary pattern between the two techniques, the NVC and nailfold D-OCT. NVC images (left images) and corresponding D-OCT en-face views (right images). Representative images of NVC pattern of the five groups—(**a**) HC and patients with SSc with (**b**) normal/nonspecific, (**c**) early, (**d**) active, and (**e**) late NVC patterns—and (**f**) coexistence of abnormal shapes and giant capillaries in a patient with active NVC pattern (left images) and corresponding D-OCT en-face views (right images). The images illustrate the correspondence of capillary loops, their distribution, their morphology, the presence of hemorrhages, and the overall capillary pattern between the NVC and nailfold D-OCT. D-OCT, dynamic optical coherence tomography; HC, healthy control; NVC, nailfold videocapillaroscopy; SSc, systemic sclerosis.

Limitations of this study included a lack of statistical significance of MVFD between the different specific NVC patterns. This is likely related to the pilot nature of the study, including a small number of subjects in each group; indeed, a clear trend of MVFD reduction was evident from normal/nonspecific to early, active, and late NVC patterns, and MVFD was significantly lower in patients with a higher semiquantitative NVC score, with a higher number of abnormal shapes, and with a lower number of capillaries at nail fold. In addition, we quantified the MVFD using a software tool provided by the producer, whereas novel image processing methodologies are currently ongoing to enhance the technical capabilities of D-OCT for the accurate detection and characterization of microcirculation in the skin (Zugaj et al., 2018).

Most importantly, although our results offer a preliminary validation of MVFD at the nail fold, the application to other skin areas in SSc should be explored. Future studies should also include other positive control groups, such as those with dermatomyositis, to explore the specificity of the technique. Furthermore, the assessment of its sensitivity to change over time is needed to validate MVFD as an outcome measure. The assessment of D-OCT MVFD in a second independent, longitudinal validation study and in the context of randomized controlled trials is currently ongoing and will offer definitive answers on its use as an endpoint for microvascular skin involvement.

MATERIALS AND METHODS

Patients

A total of 50 subjects were consecutively enrolled in this prospective study between August 2016 and March 2017. First, four groups of 10 consecutive patients with SSc, each with one of the four NVC patterns described below, were enrolled from the Outpatient Clinic at Chapel Allerton Hospital (Leeds, United Kingdom). Once we determined their age range and sex ratios, we sought to recruit a fifth group of 10 age- and sex-matched HCs from the staff. All patients with SSc fulfilled the 2013 American College of Rheumatology/

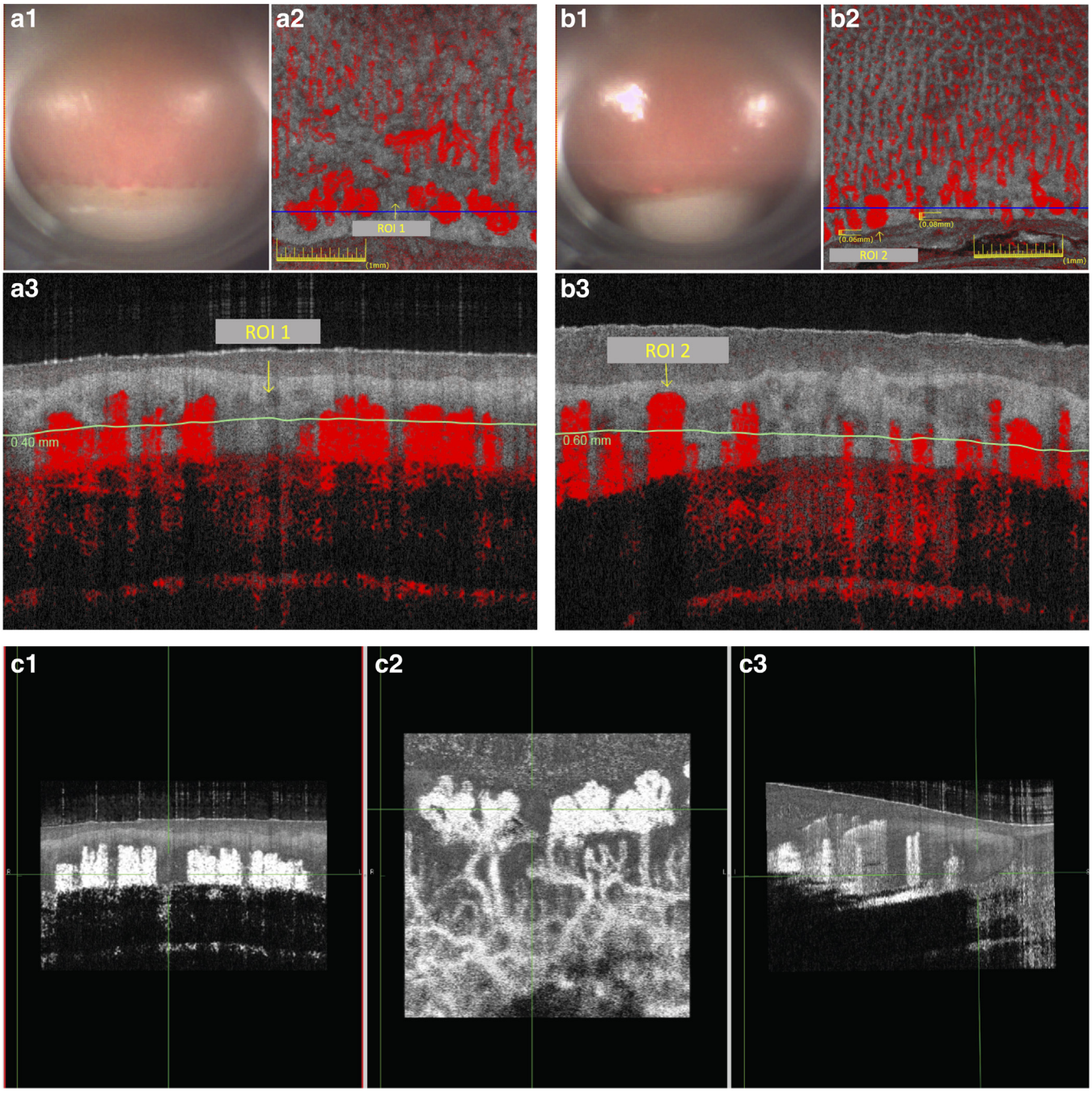

Figure 2. D-OCT provides a virtual vascular biopsy of the examined nailfold, amenable to different type of quantitative analysis, in particular it is able to measure ROI and each capillary parameter and to provide a three planes-view of the examined sample. (**a–c**) Two representative nailfold areas scanned by D-OCT. a1 and b1 show the site of analysis visualized at the PC screen through the probe. a2 and b2 show the en-face view of nailfold D-OCT, where it is possible, to visualize the capillary pattern to analyze and measure each capillary parameter such as capillary loops and distance between structures. Representative ROIs 1 and 2 are shown in two different views (enface a2 and b2 and cross-sectional in a3 and b3). ROI 1 does not show a dynamic signal, whereas ROI 2 shows a giant capillary. c1, c2, and c3 show the three-plane views of the representative examined nailfold. Altogether, the slices collected for each examined site provide a virtual vascular biopsy of the sample, amenable to different types of quantitative analysis. D-OCT, dynamic optical coherence tomography; PC, computer; ROI, region of interest.

European League Against Rheumatism classification criteria (van den Hoogen et al., 2013). Subjects were asked not to drink coffee or tea or smoke on the day of the assessment. Patients with arterial hypertension, diabetes, or other vascular diseases were excluded. The United Kingdom Health Research Authority approved the study, and written informed consent was obtained from each subject within the STRIKE SSc (STratification for RisK of progrEssion in SSc) registry (Research and Development:15/071; Integrated Research Approval System:178638; sponsor reference: RR11/071). Demographic and clinical data were collected at the time of D-OCT scans and included a wide set of variables, as previously described (Abignano et al., 2019a, 2014).

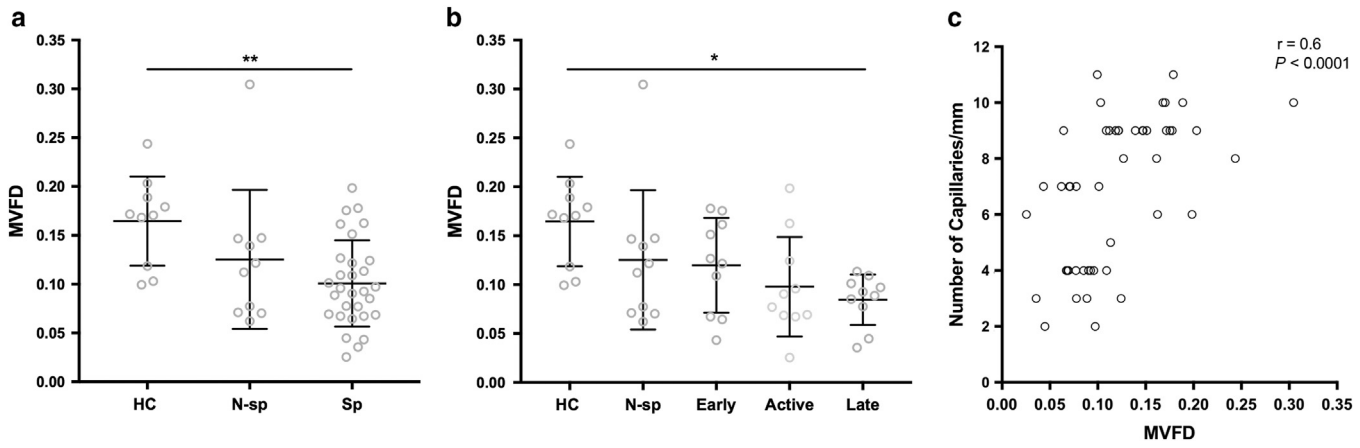

Figure 3. Skin MVFD by D-OCT at nailfold is significantly different between the NVC pattern groups and correlates with the quantitative analysis of NVC. (**a**) Quantitative analysis of MVFD across the three groups—HCs and patients with SSc with N-Sp and SSc with Sp NVC patterns. Data are shown as mean and SD. (ANOVA test, $^{**}P < 0.005$). (**b**) Comparison of MVFD in the five groups, including the three specific NVC patterns (HC, N-Sp, early, active, late). Data are shown as mean and SD (ANOVA test, $^{*}P < 0.05$). (**c**) Pearson's correlation analysis between MVFD and the number of capillaries/mm. HC, healthy control; MVFD, microvascular flow density; N-Sp, normal/nonspecific; NVC, nailfold videocapillaroscopy; Sp, specific; SSc, systemic sclerosis.

NVC

Each patient within the STRIKE SSc registry has NVC performed at eight fingers every 12 months by a trained assessor (LG). Patients were acclimatized to room temperature for 15–20 minutes before NVC examination. A small drop of immersion oil is placed on the nail beds of the eight fingers (excluding the thumbs), and the nailfold capillaries are examined by NVC (Optilia, Mediscope-Digital Video Microscope, Optilia Instruments AB, Sollentuna, Sweden). NVC patterns are determined as normal or nonspecific (i.e., presence of enlarged loops and/or hemorrhages), or as early, active, or late SSc patterns (Cutolo et al., 2000). A total of 10 patients with SSc with normal/nonspecific, 10 with early, 10 with active, and 10 with late NVC patterns, matched by age and sex, were consecutively selected from the Outpatient Clinic. The capillary score of six parameters (presence of enlarged capillaries, presence of giant capillaries, microhemorrhages, loss of capillaries, disorganization of the microvascular array, and abnormal shapes) is usually made using a semiquantitative rating scale according to the previous studies (0 = no changes, 1 = <33% of capillary alterations/reduction, 2 = 33–66% of capillary alterations/reduction, 3 = >66% of capillary alterations/reduction, per linear mm) and considering the average of the eight fingers of each parameter (Sulli et al., 2008). However, for the purpose of this study, for each patient, the finger with the highest score (i.e., the most affected), that is, the sum of the six parameters, was selected and underwent NVC additional scoring and D-OCT imaging.

In patients classified as SSc but without a scleroderma NVC pattern, the finger showing the most nonspecific abnormalities (i.e., percentage of enlarged loops and/or microhemorrhages) was selected. For the selected finger, semiquantitative and quantitative NVC scoring was carried out, and the results were compared with those of the D-OCT scoring. In detail, the microangiopathy evolution score, the sum of three scores for loss of capillaries, disorganization of the microvascular array, and abnormal shapes (range = 0–9) was calculated as semiquantitative NVC score (Sulli et al., 2008). Quantitative assessment of NVC images consisted of counting per linear mm the following four capillaroscopic parameters within the distal row of the nail fold: number of capillaries, giant capillaries, microhemorrhages, and abnormal shapes (Avouac et al., 2017; Cutolo et al., 2016).

A fifth group of 10 HCs, matched by age and sex to NVC groups, was subsequently recruited from the staff and underwent NVC as described. The finger with the highest capillary score of patients with SSc and the fourth finger of the dominant hand of subjects with the normal capillary pattern were subsequently analyzed by D-OCT. NVC images were collected at ×50 magnification to obtain a wider view of the nail bed and to be matched with D-OCT images. Images were subsequently scored according to the ×200 magnification using a calibration ruler. Semiquantitative and quantitative NVC scoring of the selected finger was then compared with that of the D-OCT imaging of the same sites of analysis.

Dynamic OCT and postprocessing analysis

A total of 50 nail folds were scanned the same day, after NVC assessment, using the VivoSight scanner equipped with a 20-kHz swept-source laser and D-OCT processing software (Michelson Diagnostics, Maidstone, United Kingdom). The tool provides an indirect measure of blood flow in the D-OCT scans by calculating the signal intensity of speckle variance across all frames at different depths, providing an arbitrary measure of blood flow that corresponds to the proportion of image pixels in which movement is detected (Olsen et al., 2018a; Themstrup et al., 2016a). An illustration explaining the D-OCT procedure and its characteristics can be found on the manufacturer's website (https://vivosight.com/vivosight-dx/).

Each scan included 500 frames with a width of 3 mm and lasted 60 seconds. The capillary pattern was visualized in horizontal D-OCT images (en-face view). The operator performing the D-OCT scans, blinded to NVC results, classified the capillary pattern (normal/nonspecific, early, active, late) of the scanned digit analyzing the D-OCT en face-view images. All the D-OCT images were collected by an operator (GA) blinded to NVC results and were subsequently analyzed by the built-in software tool (Michelson Diagnostics) to extract a quantitative measure of the signal across all frames in 0.01 mm intervals in the D-OCT images using a previously reported methodology (Themstrup et al., 2016b). OCT Analyse software permitted following the curved surface of the skin, ensuring that the whole area of the horizontal image was viewed at the same

depth below the skin surface as described by Themstrup et al. (2016b). The mean value of the D-OCT signal from 0.2 to 0.6 mm depth below the skin surface for each D-OCT scan was calculated and defined as MVFD.

To measure the D-OCT reliability, seven participants (two HCs and five patients with SSc) underwent repeat evaluations of the nail fold by two different assessors (GA and SE) in the same scanning session. Six subjects (one HC and five patients with SSc) were evaluated by the assessor 1 (GA) a week apart to measure intra-observer reliability.

Statistics

The normal distribution of each parameter was verified by the D'Agostino and Pearson omnibus normality test. Continuous variables were expressed as mean ± SD (if normally distributed) and as median (interquartile range) (if not normally distributed); and categorical data were expressed as number and percentage. ANOVA and trend tests were used to perform a comparison between the groups. The strength of monotonic relationship between parameters was calculated using Pearson's correlation test. Intraclass correlation coefficient with 95% confidence interval was calculated to estimate the intraobserver and interobserver reliability. A $P < 0.05$ was considered statistically significant. Statistical analysis was carried out using GraphPad Prism software, version 7.0 (GraphPad Software, San Diego, CA), and Statistical Package for the Social Sciences software, version 26 (SPSS, Chicago, IL).

Data availability statement

Datasets related to this article (raw data of the graphs) are available at https://www.sclerodermaprogram.co.uk/publications hosted at https://www.sclerodermaprogram.co.uk/

ORCIDs

Giuseppina Abignano: http://orcid.org/0000-0002-1479-0133
Lorraine Green: http://orcid.org/0000-0003-1620-2443
Sookhoe Eng: http://orcid.org/0000-0002-5265-8897
Paul Emery: http://orcid.org/0000-0002-7429-8482
Francesco Del Galdo: http://orcid.org/0000-0002-8528-2283

CONFLICT OF INTEREST

The authors state no conflict of interest.

ACKNOWLEDGMENTS

The study was supported by Career Development Fellowship funding to FDG, Cheney Translational Skin Science Facility, and the National Institute for Health Research Biomedical Research Centre.

AUTHOR CONTRIBUTIONS

Conceptualization: GA, FDG; Data Curation: GA, LG, SE, FDG; Formal Analysis: GA, LG, FDG; Funding Acquisition: PE, FDG; Investigation: GA, LG, SE; Methodology: GA, PE, FDG; Project Administration: GA, SE, FDG; Resources: GA, LG, SE, PE, FDG; Software: GA, LG, SE, PE, FDG; Supervision: GA, FDG; Validation: GA, PE, FDG; Visualization: GA, LG, SE, PE, FDG; Writing - Original Draft Preparation: GA; Writing - Review and Editing: GA, LG, SE, PE, FDG

Disclaimer

The views expressed are those of the authors and not necessarily those of the National Health Service, the National Institute for Health Research, or the Department of Health. The funders had no role in study design, data collection and analysis, decision to publish the study, or preparation of the manuscript.

REFERENCES

Abignano G, Aydin SZ, Castillo-Gallego C, Liakouli V, Woods D, Meekings A, et al. Virtual skin biopsy by optical coherence tomography: the first quantitative imaging biomarker for scleroderma. Ann Rheum Dis 2013;72:1845–51.

Abignano G, Blagojevic J, Bissell LA, Dumitru RB, Eng S, Allanore Y, et al. European multicentre study validates enhanced liver fibrosis test as biomarker of fibrosis in systemic sclerosis. Rheumatology (Oxford) 2019a;58:254–9.

Abignano G, Cuomo G, Buch MH, Rosenberg WM, Valentini G, Emery P, et al. The enhanced liver fibrosis test: a clinical grade, validated serum test, biomarker of overall fibrosis in systemic sclerosis. Ann Rheum Dis 2014;73:420–7.

Abignano G, Del Galdo F. Quantitating skin fibrosis: innovative strategies and their clinical implications. Curr Rheumatol Rep 2014;16:404.

Abignano G, Del Galdo F. Biomarkers as an opportunity to stratify for outcome in systemic sclerosis. Eur J Rheumatol 2020;7(Suppl. 3):S193–202.

Abignano G, Kapadia A, Lettieri G, Goodfield M, Emery P, McGonagle D, et al. Use of optical coherence tomography for the diagnosis of preclinical lesions of circumscribed palmar hypokeratosis. Clin Exp Dermatol 2017;42:192–5.

Abignano G, Laws P, Del Galdo F, Marzo-Ortega H, McGonagle D. Three-dimensional nail imaging by optical coherence tomography: a novel biomarker of response to therapy for nail disease in psoriasis and psoriatic arthritis. Clin Exp Dermatol 2019b;44:462–5.

An L, Qin J, Wang RK. Ultrahigh sensitive optical microangiography for in vivo imaging of microcirculations within human skin tissue beds. Opt Express 2010;18:8220–8.

Avouac J, Fransen J, Walker UA, Riccieri V, Smith V, Muller C, et al. Preliminary criteria for the very early diagnosis of systemic sclerosis: results of a Delphi Consensus Study from EULAR Scleroderma Trials and Research Group. Ann Rheum Dis 2011;70:476–81.

Avouac J, Lepri G, Smith V, Toniolo E, Hurabielle C, Vallet A, et al. Sequential nailfold videocapillaroscopy examinations have responsiveness to detect organ progression in systemic sclerosis. Semin Arthritis Rheum 2017;47:86–94.

Aydin SZ, Castillo-Gallego C, Ash ZR, Abignano G, Marzo-Ortega H, Wittmann M, et al. Potential use of optical coherence tomography and high-frequency ultrasound for the assessment of nail disease in psoriasis and psoriatic arthritis. Dermatology 2013;227:45–51.

Barsotti S, d'Ascanio A, Valentina V, Chiara S, Silvia B, Laura A, et al. Is there a role for laser speckle contrast analysis (LASCA) in predicting the outcome of digital ulcers in patients with systemic sclerosis? Clin Rheumatol 2020;39:69–75.

Bissell LA, Abignano G, Emery P, Del Galdo F, Buch MH. Absence of Scleroderma pattern at nail fold capillaroscopy valuable in the exclusion of Scleroderma in unselected patients with Raynaud's phenomenon. BMC Musculoskelet Disord 2016;17:342.

Bukhari M, Hollis S, Moore T, Jayson MI, Herrick AL. Quantitation of microcirculatory abnormalities in patients with primary Raynaud's phenomenon and systemic sclerosis by video capillaroscopy. Rheumatology (Oxford) 2000;39:506–12.

Caramaschi P, Canestrini S, Martinelli N, Volpe A, Pieropan S, Ferrari M, et al. Scleroderma patients nailfold videocapillaroscopic patterns are associated with disease subset and disease severity. Rheumatology (Oxford) 2007;46:1566–9.

Choi WJ, Reif R, Yousefi S, Wang RK. Improved microcirculation imaging of human skin in vivo using optical microangiography with a correlation mapping mask. J Biomed Opt 2014;19:36010.

Cutolo M, Herrick AL, Distler O, Becker MO, Beltran E, Carpentier P, et al. Nailfold videocapillaroscopic features and other clinical risk factors for digital ulcers in systemic sclerosis: a multicenter, prospective cohort study. Arthritis Rheumatol 2016;68:2527–39.

Cutolo M, Sulli A, Pizzorni C, Accardo S. Nailfold videocapillaroscopy assessment of microvascular damage in systemic sclerosis. J Rheumatol 2000;27:155–60.

Cutolo M, Vanhaecke A, Ruaro B, Deschepper E, Ickinger C, Melsens K, et al. Is laser speckle contrast analysis (LASCA) the new kid on the block in systemic sclerosis? A systematic literature review and pilot study to evaluate reliability of LASCA to measure peripheral blood perfusion in scleroderma patients. Autoimmun Rev 2018;17:775–80.

Deegan AJ, Talebi-Liasi F, Song S, Li Y, Xu J, Men S, et al. Optical coherence tomography angiography of normal skin and inflammatory dermatologic conditions. Lasers Surg Med 2018;50:183–93.

Della Rossa A, Cazzato M, d'Ascanio A, Tavoni A, Bencivelli W, Pepe P, et al. Alteration of microcirculation is a hallmark of very early systemic sclerosis patients: a laser speckle contrast analysis. Clin Exp Rheumatol 2013;31(Suppl. 76):109–14.

Kang T, Abignano G, Lettieri G, Wakefield RJ, Emery P, Del Galdo F. Skin imaging in systemic sclerosis. Eur J Rheumatol 2014;1:111–6.

LeRoy EC, Medsger TA Jr. Criteria for the classification of early systemic sclerosis. J Rheumatol 2001;28:1573–6.

Maricq HR, LeRoy EC, D'Angelo WA, Medsger TA Jr, Rodnan GP, Sharp GC, et al. Diagnostic potential of in vivo capillary microscopy in scleroderma and related disorders. Arthritis Rheum 1980;23:183–9.

Melsens K, Van Impe S, Paolino S, Vanhaecke A, Cutolo M, Smith V. The preliminary validation of laser Doppler flowmetry in systemic sclerosis in accordance with the OMERACT filter: a systematic review. Semin Arthritis Rheum 2020;50:321–8.

Olsen J, Birch-Johansen FH, Themstrup L, Holmes J, Jemec GBE. Dynamic optical coherence tomography of histamine induced wheals. Skin Res Technol 2018a;24:592–8.

Olsen J, Holmes J, Jemec GBE. Advances in optical coherence tomography in dermatology-a review. J Biomed Opt 2018b;23:1–10.

Pires NSM, Dantas AT, Duarte ALBP, Amaral MM, Fernandes LO, Dias TJC, et al. Optical coherence tomography as a method for quantitative skin evaluation in systemic sclerosis. Ann Rheum Dis 2018;77:465–6.

Riccieri V, Vasile M, Iannace N, Stefanantoni K, Sciarra I, Vizza CD, et al. Systemic sclerosis patients with and without pulmonary arterial hypertension: a nailfold capillaroscopy study. Rheumatology (Oxford) 2013;52:1525–8.

Ring HC, Mogensen M, Hussain AA, Steadman N, Banzhaf C, Themstrup L, et al. Imaging of collagen deposition disorders using optical coherence tomography. J Eur Acad Dermatol Venereol 2015;29:890–8.

Ring HC, Themstrup L, Banzhaf CA, Jemec GB, Mogensen M. Dynamic optical coherence tomography capillaroscopy: a new imaging tool in autoimmune connective tissue disease. JAMA Dermatol 2016;152:1142–6.

Rosato E, Molinaro I, Rossi C, Pisarri S, Salsano F. The combination of laser Doppler perfusion imaging and photoplethysmography is useful in the characterization of scleroderma and primary Raynaud's phenomenon. Scand J Rheumatol 2011;40:292–8.

Silva I, Teixeira A, Oliveira J, Almeida I, Almeida R, Águas A, et al. Endothelial dysfunction and nailfold videocapillaroscopy pattern as predictors of digital ulcers in systemic sclerosis: a cohort study and review of the literature. Clin Rev Allergy Immunol 2015;49:240–52.

Smith V, Herrick AL, Ingegnoli F, Damjanov N, De Angelis R, Denton CP, et al. Standardisation of nailfold capillaroscopy for the assessment of patients with Raynaud's phenomenon and systemic sclerosis. Autoimmun Rev 2020;19:102458.

Smith V, Vanhaecke A, Herrick AL, Distler O, Guerra MG, Denton CP, et al. Fast track algorithm: how to differentiate a "scleroderma pattern" from a "non-scleroderma pattern". Autoimmun Rev 2019;18:102394.

Su P, Cao T, Tang MB, Tey HL. In vivo high-definition optical coherence tomography: a bedside diagnostic aid for morphea. JAMA Dermatol 2015;151:234–5.

Sulli A, Secchi ME, Pizzorni C, Cutolo M. Scoring the nailfold microvascular changes during the capillaroscopic analysis in systemic sclerosis patients. Ann Rheum Dis 2008;67:885–7.

Themstrup L, Ciardo S, Manfredi M, Ulrich M, Pellacani G, Welzel J, et al. In vivo, micro-morphological vascular changes induced by topical brimonidine studied by dynamic optical coherence tomography. J Eur Acad Dermatol Venereol 2016a;30:974–9.

Themstrup L, Welzel J, Ciardo S, Kaestle R, Ulrich M, Holmes J, et al. Validation of Dynamic optical coherence tomography for non-invasive, in vivo microcirculation imaging of the skin. Microvasc Res 2016b;107:97–105.

Ulrich M, Themstrup L, de Carvalho N, Ciardo S, Holmes J, Whitehead R, et al. Dynamic optical coherence tomography of skin blood vessels - proposed terminology and practical guidelines. J Eur Acad Dermatol Venereol 2018;32:152–5.

Ulrich M, Themstrup L, de Carvalho N, Manfredi M, Grana C, Ciardo S, et al. Dynamic optical coherence tomography in dermatology. Dermatology 2016;232:298–311.

van den Hoogen F, Khanna D, Fransen J, Johnson SR, Baron M, Tyndall A, et al. 2013 classification criteria for systemic sclerosis: an American College of Rheumatology/European league against rheumatism collaborative initiative. Ann Rheum Dis 2013;72:1747–55.

Varga J, Trojanowska M, Kuwana M. Pathogenesis of systemic sclerosis: recent insights of molecular and cellular mechanisms and therapeutic opportunities. J Scleroderma Relat Disord 2017;2:137–52.

Welzel J, Lankenau E, Birngruber R, Engelhardt R. Optical coherence tomography of the human skin. J Am Acad Dermatol 1997;37:958–63.

Zugaj D, Chenet A, Petit L, Vaglio J, Pascual T, Piketty C, et al. A novel image processing workflow for the in vivo quantification of skin microvasculature using dynamic optical coherence tomography. Skin Res Technol 2018;24:396–406.